THE JOURNAL OF BIOLOGICAL CHEMISTRY VOL. 286, NO. 11, pp. 9127–9135, March 18, 2011

Kallikrein-5 Promotes Cleavage of Desmoglein-1 and Loss of Cell-Cell Cohesion in Oral Squamous Cell Carcinoma*

Received for publication, October 5, 2010, and in revised form, November 24, 2010 Published, JBC Papers in Press, December 16, 2010, DOI 10.1074/jbc.M110.191361

Rong Jiang[‡1], **Zonggao Shi**[‡], **Jeffrey J. Johnson**[‡], **Yueying Liu**[‡], **and M. Sharon Stack**[‡§2]

From the [‡]*Department of Pathology and Anatomical Science and* [§]*Medical Pharmacology & Physiology, University of Missouri School of Medicine, Columbia, Missouri 65212*

Oral squamous cell carcinoma (OSCC) ranks among the top 8 causes of cancer death worldwide, with only a 60% 5-year survival rate, highlighting the need for discovery of novel biomarkers and therapeutic targets. We have previously reported that expression of a panel of serine proteinase kallikreins (KLK 5, 7, 8, and 10) is correlated with formation of more aggressive OSCC tumors in a murine orthotopic OSCC model and is elevated in human OSCC. Current studies focus on understanding the potential role of KLK5 in OSCC progression. In initial studies, KLK levels in malignant OSCC cells (SCC25) were compared with cells from normal oral mucosa (OKF/6) and pre-malignant oral keratinocytes (pp126) using qPCR. A marked elevation of all KLKs was observed in aggressive SCC25 cells relative to OKF/6 cells. In normal skin, KLKs are involved in desquamation during epidermal differentiation via proteolytic cleavage of the desmosomal cadherin component desmoglein 1 (Dsg1). As loss of cell-cell cohesion is prevalent in tumor metastasis, Dsg1 integrity was evaluated. Results show that SCC25 cells exhibit cleavage of Dsg1, which is blocked by proteinase inhibitor treatment as well as by siRNA silencing of KLK5 expression. Furthermore, cell-cell aggregation assays demonstrate that silencing of KLK5 enforces cell-cell adhesion; conversely, overexpression of KLK5 in normal oral mucosal cells (OKF/6) enhances cell dispersal. These data suggest that KLK5 may promote metastatic dissemination of OSCC by promoting loss of junctional integrity through cleavage of desmoglein 1.

Oral cavity cancer results in over 200,000 deaths annually and is one of the top eight most frequently diagnosed cancers worldwide (1). The most common malignancy of the oral cavity is oral squamous cell carcinoma (OSCC),[3] including tumors affecting the tongue, floor of the mouth, buccal mucosa, lips, palate, and gingiva, causing more deaths than any other oral disease (2–3). According to National Cancer Institute statistics, about 23,110 new cases of oral cancer were diagnosed in 2009 in the United States (4). Unfortunately, despite advancements in surgery, chemotherapy, and radiation, only 60% of these individuals will survive for five years. The high mortality associated with OSCC is due primarily to the detection of late-stage disease after the primary tumor has metastasized. Treatment of advanced OSCC is also associated with high morbidity and mortality, resulting from local, regional, and distant metastasis (2–3). The cellular and biochemical factors that underlie locoregional and distant spread of the disease are poorly understood. Invasion and metastasis of OSCC require multiple cellular events including disruption of cell-cell adhesive contacts, cytoskeletal alterations, and basement membrane attachment, matrix protein proteolysis, and migration (5–6). Thus a more detailed analysis of the molecular events that contribute to OSCC metastasis is a necessary prerequisite for the development of novel early detection and treatment strategies that have a favorable impact on the survival of OSCC patients.

Human tissue kallikreins or kallikrein-related peptidases (KLKs) constitute a single family of 15 highly conserved trypsin- or chymotrypsin-like serine proteases encoded by a large uninterrupted cluster of protease-encoding genes (*KLK1–15*) co-localized on chromosome 19q13.4 (7). In initial studies, we identified expression of a panel of kallikreins (KLK-5, -7, -8, and -10) that have a marked elevation in malignant OSCC relative to normal oral mucosa and normal tongue (8). The physiologic roles and natural substrates for most KLKs have not been defined; however expression of multiple KLKs in a single tissue compartment suggests participation in proteolytic cascades (9–12). As KLK5 can auto-activate and contributes to activation of pro-KLK2, -3, -6, -7, -11, -12, and -14 zymogens, KLK5 may be considered an initiator of putative KLK proteolytic cascades (13). In normal skin, KLK5 is involved in desquamation during epidermal differentiation via proteolytic cleavage of the desmosomal cadherin component desmoglein 1(14–15).

Desmosomes are intercellular junctions that provide strong adhesion between cells. They are particularly abundant in tissues such as epithelia and cardiac muscle that are continually assailed by mechanical forces. Extracellularly, desmosomal adhesion is mediated by the desmosomal cadherins comprised of desmogleins (Dsg) and desmocollins (Dsc) (16–19). Previous studies have shown that loss of desmosomal adhesion can significantly disrupt tissue integrity (20).

In the current study, the effect of modulating KLK5 levels on the expression and integrity of desmoglein 1 (Dsg1) was evaluated in normal oral keratinocytes and OSCC cells. Our data demonstrate that malignant OSCC cells exhibit cleavage

* This work was supported, in whole or in part, by Research Grant CA085870 (to M. S. S.) from the NCI, National Institutes of Health.
[1] Present address: Dept. of Biochemistry, Emory University, Atlanta, GA.
[2] To whom correspondence should be addressed: Dept. of Pathology and Anatomical Sciences, 1 Hospital Drive, M214C Medical Sciences Bldg., University of Missouri School of Medicine, Columbia, MO 65212. E-mail: stackm@missouri.edu.
[3] The abbreviations used are: OSCC, oral squamous cell carcinoma; KLK, kallikrein; TEM, transmission electron microscopy; Dsg, desmoglein; Dsc, desmocollin.

of Dsg1 which can be blocked by treatment with proteinase inhibitors as well as by silencing of KLK5. Modification of KLK5 expression also alters cell-cell aggregation and cohesion. These results suggest KLKs may contribute to metastatic dissemination of OSCC via a mechanism involving KLK5-catalyzed Dsg1 cleavage.

EXPERIMENTAL PROCEDURES

Antibodies—Rabbit polyclonal antibodies to kallikrein 5, generated against a synthetic peptide based on the kallikrein loop area of kallikrein 5, were obtained from Abcam (Cambridge, MA). This antibody reacts with KLK5, but has no reactivity against KLKs 1–7 and 9–15. Mouse monoclonal anti-desmoglein 1 antibodies were purchased from BD Transduction Laboratories (San Jose, CA), and do not cross-react with Dsg2 or Dsg3 according to manufacturer's specifications. Mouse monoclonal anti-E-cadherin antibody was obtained from Invitrogen (Carlsbad, CA). Anti-GAPDH was purchased from Santa Cruz Biotechnology.

Immunohistochemical Analysis—Immunohistochemical analysis was performed by analyzing tongue-derived specimens of microarrayed human OSCC and normal oral tissues (US Biomax). Paraformaldehyde fixed, paraffin-embedded sections (4 μm) were de-paraffinized with xylene and rehydrated in a series of ethanol washes. Endogenous peroxidase activity was quenched with 3.3% hydrogen peroxide in methanol for 30 min. Antigen retrieval was enhanced by microwaving in 10 mM sodium citrate pH 6.0. Nonspecific binding was blocked with 3% normal horse serum in PBS for 30 min. Sections were incubated for 1 h at room temperature with primary antibody (1:15–1:25 dilution) in 1% BSA in PBS. Staining was detected using an avidin-biotin horse radish peroxidase system (Vectastain Universal Elite ABC kit, Cat. PK-6200, Vector Laboratories, Burlingame, CA), with positive cells staining brown using diaminobenzidine chromogen and hydrogen peroxide substrate (Liquid DAB substrate pack HK153-5K, BioGenex, San Ramon, CA). Analysis of tissue staining was done by light microscopy and scoring of KLK5 was assigned according to the average overall intensity of staining and was graded as follows: 0, no staining; 1, fine granular staining; 2, somewhat coarse staining; 3, very coarse staining.

Cell Culture—SCC25 cells, originally derived from squamous cell carcinoma of the tongue, were obtained from American Type Culture Collection. Telomerase reverse transcriptase-immortalized normal oral keratiocytes (OKF6/T) were the generous gift of Dr. James Rhinewald, Brigham & Women's Hospital, Harvard Institutes of Medicine (Boston, MA) (21). Premalignant oral keratinocytes (pp126 cells) were a gift from Dr. D. Oda, University of Washington (Seattle, WA) (22). SCC25 cells were routinely maintained in DMEM/F12 1:1 media containing 10% fetal calf serum and supplemented with 100 units/ml penicillin and 100 μg/ml streptomycin or in serum-free DMEM containing 1.2 mM Ca^{2+} (23). OKF/6 cells were maintained in keratinocyte-SFM (Invitrogen) supplemented with 100 units/ml penicillin, 100 μg/ml streptomycin, 0.2 ng/ml epidermal growth factor (EGF), 25 μg/ml bovine pituitary extract (BPE), and 0.4 mM $CaCl_2$. pp126 cells were maintained in keratinocyte-SFM supplemented with 100 units/ml penicillin, 100 μg/ml streptomycin, 5 ng/ml EGF, and 50 μg/ml BPE (supplied with the medium). In some experiments, cells were cultured for up to 7 days in medium containing the proteinase inhibitors leupeptin (Sigma, 100 μM final concentration) and chymostatin (Sigma, 100 μM final concentration) (24) to block KLK activity.

To generate SCC25 cells with reduced KLK5 expression (KLK5 knockdown, designated SCC25-KLK5-KD), pGFP-V-RS plasmid containing a gene-specific shRNA sequence silencing KLK5 (GTG TTG GTG CAT CCA CAG TGG CTG CTC AC) (OriGene Technologies, Rockville, MD) was used to transfect SCC25 cells using the Human Keratinocyte Nucleofector kit (Amaxa GmbH, Germany). The resulting clonal cell lines were routinely maintained in the medium described above supplemented with puromycin and were assessed for expression of KLK5 by qPCR and immunofluorescence microscopy (see below). To generate cells that overexpress KLK5 in the OKF/6 normal oral epithelial cell background (designated OKF/6-KLK5+), pCEFL-KLK5 plasmid (gift from Dr. Thomas Bugge, National Institutes of Dental and Craniofacial Research, Bethesda, MD) was used to transfect OKF cells using the Human Keratinocyte Nucleofector kit (Amaxa GmbH, Germany). The resulting clonal cell lines were routinely maintained in the medium described above supplemented with G418 and were assessed for expression of KLK5 by qPCR and immunofluorescence microscopy (see below).

Quantitative Real Time PCR (qPCR) Analysis—Total RNA was extracted with Trizol Reagent (Invitrogen) and reverse transcription was performed with 10 μg of the total RNA from each specimen using SuperScript II reverse transcriptase (Invitrogen) according to the manufacturer's protocol. The cDNA products were then diluted 1:10 and 5 μl of each were used for PCR templates. The following primer sequences were used at final concentrations of 167 nM for each: for KLK5 forward, 5′-GCA GGT AGA GAC TCC TGC CA-3′ and reverse 5′-CAC AAG GGT AAT CTC CCC AG-3′; for KLK7 forward, 5′-ACC CTC AGT GCT GGA GAA GA-3′ and reverse 5′-ACT GGG TCA AAG GTG GTG AA-3′; for KLK8 forward, 5′- AAG TGC ACC GTC TCA GGC-3′ and reverse 5′-TCC TCA CAC TTC TTC TGG-3′; for KLK10 forward, 5′-CTC TGG CGA AGC TGC TG-3′ and reverse 5′-ATA GGC TTC GGG GTC CA-3′; for Dsg1 forward, 5′-AGA TGC CTG ACT TGC GAG AT-3′ and reverse 5′-CTA TCA TGC CGG AAG TTG GT-3′; for endogenous control gene phosphoglycerate kinase (PGK) forward, 5′-GGG CTG CAT CAC CAT CAT AGG-3′ and reverse 5′-GAG AGC ATC CAC CCC AGG AAG-3′. DNA oligos were custom synthesized (Integrated DNA Technologies). Real-time PCR was performed with SYBR green Master Mix (Aplied Biosystems, Foster City, CA). PCR cycling conditions were 95 °C for 13.5 min followed by 40 cycles of 95 °C for 15 s and 60 °C for 30 s. Melt curve cycling consisted of 81 30 s cycles beginning at 55 °C increasing by 0.5 °C to 95 °C. All reactions were carried out on an iCycleriQ real-time PCR detection system (Bio-Rad). Each sample was analyzed in triplicate for each PCR measurement. Melting curves were checked to ensure specificity. Relative quantification of mRNA expression was calcu-

lated using the standard curve method with the endogenous housekeeping gene PGK level as normalizer and control sample as calibrator.

Western Blot Analysis—Cells were harvested by scraping in lysis buffer (modified RIPA buffer, with an added protease inhibitor mixture tablet) and samples were centrifuged at 6,000 rpm for 10 min at 4 °C to produce supernatant. Protein concentration of samples was determined by using a detergent compatible protein assay kit (Bio-Rad). Proteins were separated by SDS-polyacrylamide gel electrophoresis (PAGE), and then transferred onto a polyvinylidene fluoride (PVDF) microporous membranes (Millipore). After blocking nonspecific binding to membranes in 3% BSA in TBST for 1 h at room temperature, membranes were incubated with primary antibodies for 3 h at room temperature or overnight at 4 °C, and then with HRP-conjugated secondary antibodies. Immunoreactivity was determined by SuperSignal West Dura Extended Duration Substrate kit (Thermo Scientific). Blots were also probed with antibodies against GAPDH to ascertain equal protein loading. Images were acquired with Fuji Film LAS-4000 Luminescent Image Analyzer. Semi-quantitative analysis of bands was performed by densitometry to evaluate the relative optical density of bands on a given gel. The relative optical densities are expressed on an arbitrary scale.

Immunofluorescence Microscopy—Cells were placed on coverslips in 6-well dishes and were cultured to 80% confluence. Adherent cells were washed once with 37 °C phosphate-buffered saline (PBS) once and fixed with 4% paraformaldehyde in PBS containing 0.12 M Sucrose for 20 min. For intracellular antibodies, cells were permeabilized in 0.3% Triton X-100 in PBS for 5 min at room temperature. After blocking with 10% bovine serum albumin (BSA) in PBS for 1 h, the cells were labeled with primary antibodies for 1 h, followed by the respective Alexa-Fluor-labeled secondary antibodies for 30 min. Coverslips were removed from 6-well plates, air dried, and mounted to slide with Gelvatol + DABCO (sigma d2522) with the cell side face down. Specimens were examined and images were acquired with an Olympus IX81 Inverted Spinning Disk Confocal Microscope system using the widefield fluorescence function.

Transmission Electron Microscopy (TEM)—Samples were fixed using 2% glutaraldehyde and 2% paraformaldehyde in 0.1 M cacodylate buffer, washed with 0.1 M cacodylate buffer; then with 1% OsO_4, 0.8% potassium ferricyanide in 0.1 M cacodylate buffer for 30 min at room temperature for secondary fixation. After rinsing with ultra pure water, 2% aqueous uranyl acetate was used for 30 min for tertiary fixation. After washing, samples were dehydrated in ascending concentrations of EtOH followed by dehydrating with 100% acetone, then infiltrated with Epon/Spurr's Resin. The samples were embedded and polymerized overnight. Coverslips were removed using liquid nitrogen and samples were returned to the oven to complete polymerization (overnight). Ultrathin sections were cut with Reichert Ultracut R ultramicrotome and collected on celloidine-coated 100-mesh nickel grids. Thin sections were examined with a JEOL 1400 transmission electron microscope (Jeol, Tokyo, Japan).

TABLE 1
Quantitative real-time PCR analysis of KLK expression ratios in normal and malignant oral cells

	SCC25/pp126	SCC25/OKF6
KLK5	3.5	87.4
KLK7	5.0	35.4
KLK8	1.4	233.3
KLK10	0.2	9.0

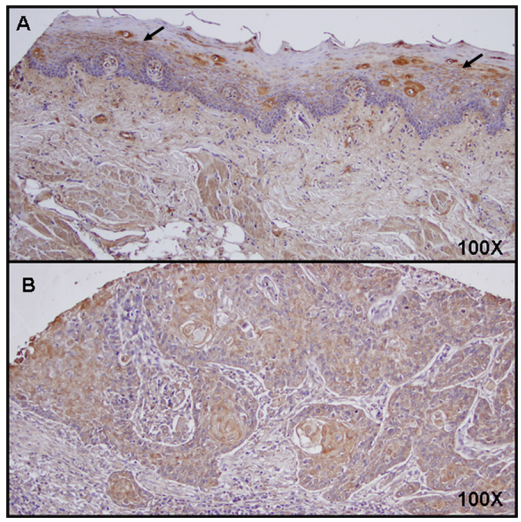

FIGURE 1. **Immunohistochemical analysis of Dsg1 expression in normal tongue and OSCC.** Sections of (*A*) normal tongue ($n = 8$) and (*B*) OSCC of the tongue ($n = 25$) were processed for immunostaining using antibodies directed against Dsg1 (1:25 dilution) followed by a biotinylated secondary antibody. Although the sample size was not sufficiently large for robust statistical power, staining trends indicate strong junctionally localized staining in normal tongue (scores: 1 = 12%, 2 = 24%, 3 = 63%), and weaker cytoplasmic staining in OSCC (scores: 1 = 56%, 2 = 35%, 3 = 8%). *Arrows* denote strong junctional Dsg1 staining. Magnification ×100.

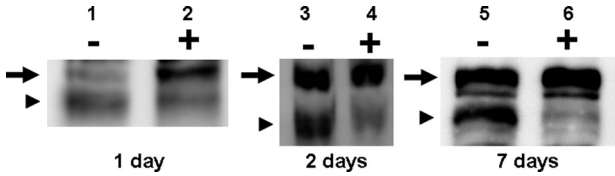

FIGURE 2. **Proteinase inhibitors block Dsg1 processing.** SCC25 cells were cultured in the absence (*lanes 1, 3, 5*) or presence (*lanes 2, 4, 6*) of leupeptin (100 μM) and chymostatin (100 μM) for 1, 2, or 7 days prior to lysis and electrophoresis on 9% SDS-polyacrylamide gels. Proteins were transferred to PVDF membrane and immunoblotted with anti-Dsg1 (1:1000) followed by peroxidase-conjugated secondary antibody (1:4000) and SuperSignal West Dura Extended Duration substrate. *Arrows* denote migration position of full-length Dsg1 (165 kDa); *arrowheads* denote migration position of cleavage product (~130 kDa).

Cell Aggregation Assay—Semi-quantitative analysis of cell-cell aggregation was performed by monitoring aggregation of single-cell suspensions as previously described (25). Cells were grown in 100-mm dishes and removed from the substrate with 0.5% EDTA in PBS. The cells were then counted, rinsed in PBS+ containing 0.5% BSA, and incubated in single-cell suspension (5×10^5 cells/ml) in culture medium containing 15 mM HEPES and 0.5% BSA. Cell suspensions were then placed in 1.5 ml Eppendorf tubes and rotated at 37 °C. At various time points up to 7 h, samples (50 μl) were removed and phase-contrast photomicrographs of living cell suspensions obtained. The number of single cells was enumerated and compared with the number obtained at the initial time point.

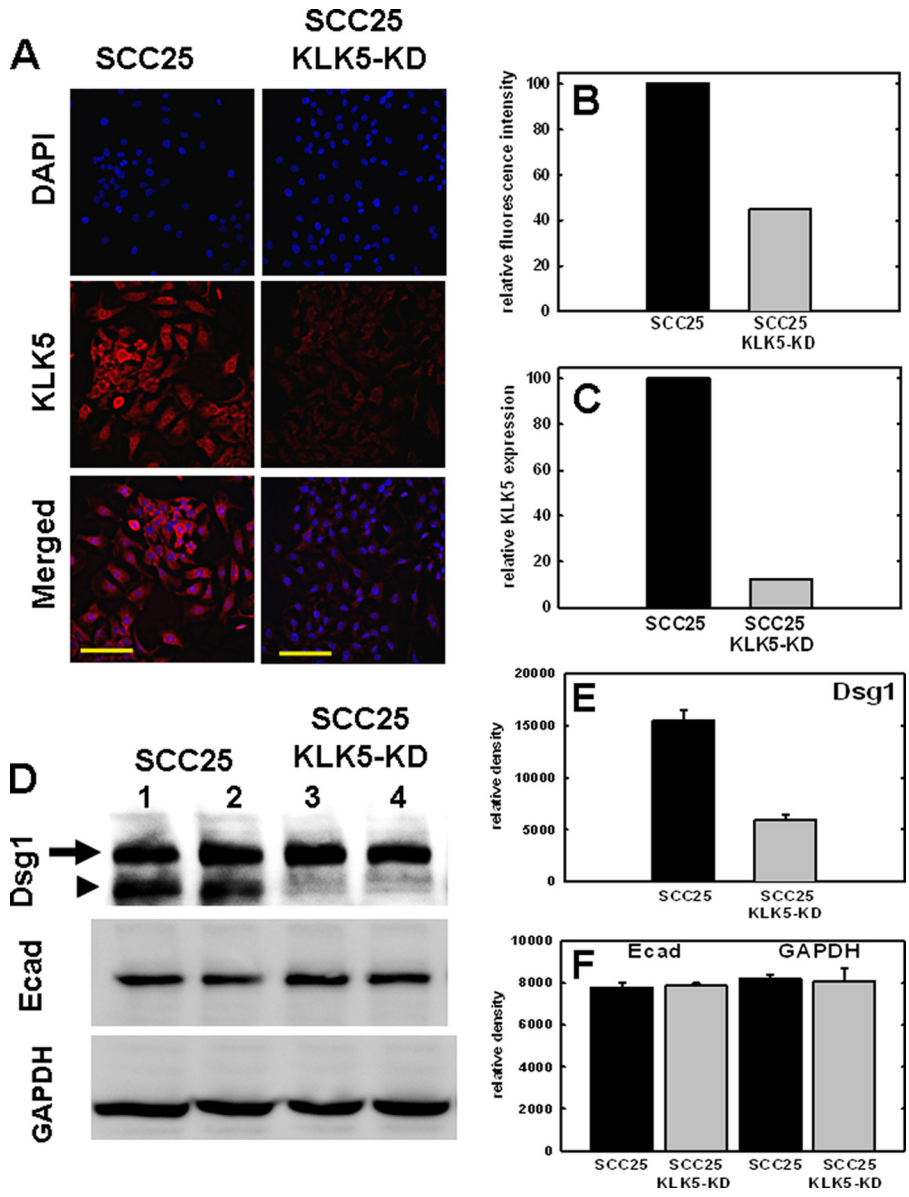

FIGURE 3. **Knockdown of KLK-5 expression reduces processing of Dsg1.** *A*, immunocytochemical analysis of KLK5 expression in control (*left panel*) or KLK5-KD (*right panel*) SCC25 cells. Cells were cultured on glass coverslips, fixed and incubated with antibodies against KLK5 (1:50 dilution) followed by Alexa-Fluor-labeled secondary antibodies and counterstained with DAPI. Yellow scale bar, 100 μm. *B*, quantification of immunofluorescent staining with NIH ImageJ for average intensity. *C*, quantitative real time PCR analysis of KLK5 levels in control and KLK5-KD SCC25 cells. Relative quantification normalized against the housekeeping gene PGK-1 mRNA levels. Graph depicts KLK5 levels in SCC25-KLK5-KD cells normalized relative to SCC25 parental cells (designated as 100). *D*, analysis of Dsg1 processing in SCC25-KLK5-KD cells. Lysates from duplicate cultures of parental SCC25 cells (*lanes 1* and *2*) or two clones of SCC25-KLK5-KD cells (*lanes 3* and *4*) were electrophoresed on 9% SDS-polyacrylamide gels, transferred to PVDF membrane and immunoblotted with anti-Dsg1 (1:1000; *upper panel*), anti-E-cadherin (1:1000; *middle panel*), or anti-GAPDH (1:4000; *lower panel*) followed by peroxidase-conjugated secondary antibody (1:4000) and peroxidase substrate. *Arrow* denotes migration position of full-length Dsg1 (165 kDa); *arrowhead* denotes migration position of cleavage product (~130 kDa). *E*, densitometric quantitation of band density of Dsg1 cleavage product denoted by *arrowhead* in *D*. *F*, densitometric quantitation of band density of corresponding blots shown in *D*.

Statistical analysis (two-tailed Student's *t* test) was performed on the mean number of the percentage of single cells from triplicate cultures and the results shown are representative of at least three independent experiments. Results are also shown as bar graphs representing the percentage of the sampled population of aggregates present in three distinct cell cluster categories (<10 cells, 10–50 cells, >50 cells), displayed as a percentage of the total population.

Dispase-based Dissociation Assay—Relative dissociation of cell-cell adherent monolayers was evaluated using a dispase-based dissociation assay as previously described (26). Paired cell lines for analysis (SCC25 and SCC25-KLK5-KD cells; or OKF/6 and OKF/6-KLK5+) were cultured in triplicate in 60-mm dishes to 80% confluence, washed twice with PBS and then incubated in 2 ml of dispase for 30 min to release cells as a monolayer. Following careful washing with PBS, cell sheets were transferred to 15 ml conical tubes in a final volume of 5 ml PBS and were subjected to 50 inversion cycles using a rocking platform. The resulting cellular fragments were placed in tissue culture plates and the number of fragments (irrespective of fragment size) was enumerated. Statistical analysis (two-tailed Student's *t* test) was performed on the

mean number of fragments from triplicate cultures and the results shown are representative of at least three independent experiments.

RESULTS

Expression of Kallikreins in Normal and Malignant Oral Cells—Microarray-based profiling of aggressive OSCC identified a panel of serine proteinase KLKs (KLK-5, -7, -8, and -10) that are highly expressed in poorly differentiated murine OSCC tumors and are abundant in human OSCC (8, 27). To evaluate the potential function of KLKs in OSCC progression, KLK gene expression levels in malignant OSCC cells (SCC25) were compared with cells from normal oral mucosa (OKF/6) and pre-malignant oral keratinocytes cells (pp126) using real time qPCR. A significant elevation of all four KLKs was observed in SCC25 cells relative to OKF/6 (Table 1). With the exception of KLK10, expression of all four KLKs was also higher in SCC25 relative to pre-malignant pp126 (Table 1).

Expression and Processing of Desmoglein 1 (Dsg1) in Normal and Malignant Oral Cells and Tissues—In stratified epithelia, strong junctional staining for Dsg1 is found in the more differentiated upper layers (Fig. 1*A*, *arrows*, 63% strong positive) (28–29), while both overall staining and junctional localization are reduced in OSCC (Fig. 1*B*, 8% strong positive) (30–31). In normal skin, numerous studies have supported a role for KLK-mediated proteolysis of Dsg1 in the cellular desquamation process in the human stratum corneum (32–35), suggesting that KLKs may play a role in loss of cellular cohesion seen in aggressive tumors. Indeed, analysis of Dsg1 by Western blotting of SCC25 whole cell lysates shows the presence of both full-length (165 kDa) Dsg1 as well as a lower molecular mass Dsg1-immunoreactive band migrating at 130 kDa (Fig. 2, *lanes 1*, *3*, and *5*). Cells cultured for 7 days with chymostatin and leupeptin, inhibitors that block KLK5 and KLK7 activities (36–38), exhibited only the 165 kDa Dsg1 protein (Fig. 2, *lanes 2*, *4*, and *6*), suggesting that the 130 kDa species represents a proteolytic Dsg1 degradation product.

Silencing of KLK5 Modulates Dsg1 Cleavage and Desmosome Formation—To evaluate the effect of altered KLK5 expression on Dsg1 cleavage, KLK5 expression was silenced in SCC25 cells using shRNA (designated SCC25-KLK5-KD). Down-regulation of KLK5 was confirmed using immunofluorescence microscopy and qPCR, showing a 60–85% knockdown of expression (Fig. 3, *A–C*). Examination of Dsg1 integrity by Western blotting shows a significant loss of the Dsg1 cleavage fragment in SCC25-KLK5-KD cells (Fig. 3*D*, *lanes 3* and *4*; Fig. 3*E*) relative to parental SCC25 cells (Fig. 3*D*, *lanes 1* and *2*). Controls show that the classic cadherin E-cadherin is not differentially processed in response to KLK-5 modification (Fig. 3, *D*, *middle panel* and *F*). GAPDH blots demonstrate equal protein loading (Fig. 3*D*, *lower panel* and *F*).

To evaluate whether cleavage of Dsg1 results in altered ultrastructural integrity, TEM was used to examine cell-cell junctions and the number of desmosomes/field in parental SCC25 *versus* SCC25-KLK5-KD cell images was enumerated. While electron dense desmosomal cadherin plaques are relatively rare in the cell-cell junctions of SCC25 cells (Fig. 4*A*). SCC25-KLK5-KD cells form abundant desmosomal contacts

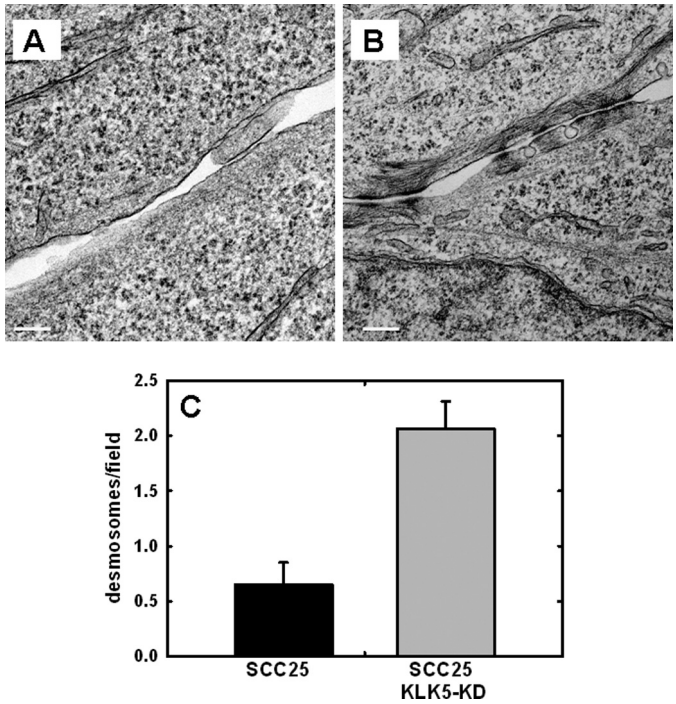

FIGURE 4. **Ultrastructural analysis of desmosomes.** SCC25 or SCC25-KLK5-KD cells were grown on coverslips to confluence, then fixed and processed for transmission electron microscopy. Ultrathin sections were examined with a JEOL 1400 Transmission Electron Microscope. Representative TEM image from (*A*) SCC25 and (*B*) SCC25-KLK5-KD cells. Scale bar, 0.2 μm. *C*, quantitation of desmosome number/field from a minimum of 70 images each of SCC25 and SCC25-KLK5-KD cells.

(Fig. 4*B*). Quantitative analysis shows SCC25 cells form 0.65 desmosome clusters per field, whereas SCC25-KLK5-KD cells form 2.06 demosome clusters per field, indicating that reducing KLK5 expression results in a 3-fold increase in desmosome number (Fig. 4*B*).

Overexpression of KLK5 Induces Dsg1 Cleavage in Normal Oral Mucosal Cells—To evaluate whether induced expression of KLK5 can initiate Dsg1 cleavage, KLK5 expression was increased in OKF/6 normal oral mucosal cells (designated OKF/6-KLK5+). Up-regulation of KLK5 was confirmed using immunofluorescence microscopy and qPCR (Fig. 5, *A–C*). Examination of Dsg1 integrity by Western blotting demonstrates the appearance of the 130 kDa Dsg1 cleavage product in KLK5-transfected OKF/6 cells (Fig. 5, *D*, *lane 3* and *E*) whereas only intact 165 kDa Dsg1 is observed in parental and vector-transfected cells (Fig. 5, *D*, *lanes 1–2* and *E*). Controls show that the classic cadherin E-cadherin is not differentially processed in response to KLK-5 modification (Fig. 5, *D*, *middle panel* and *F*). GAPDH blots demonstrate equal protein loading (Fig. 5, *D*, *lower panel* and *F*).

Modulation of KLK5 Expression Alters Cell-Cell Aggregation Kinetics and Monolayer Dissociation—In normal keratinocytes, the formation of functional intercellular adhesion complexes is dependent upon the relative expression and function of desmosomal cadherins (25–26). As the results above demonstrate a loss of Dsg1 structural integrity and reduced desmosomal cadherin number in cells expressing KLK5, the potential functional consequences of altered desmosomal integrity on cell-cell aggregation dynamics was evaluated. Ro-

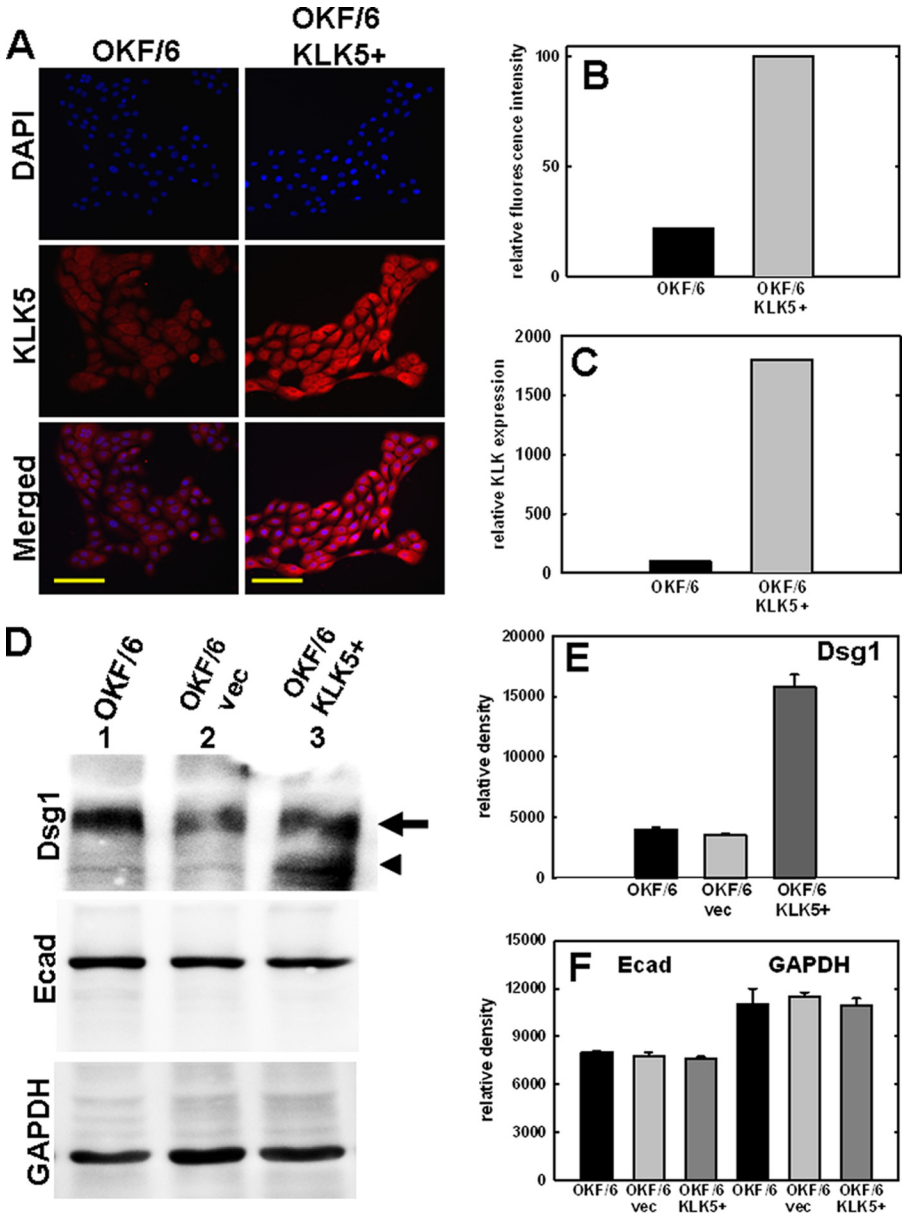

FIGURE 5. **Overexpression of KLK-5 expression induces processing of Dsg1.** *A*, immunocytochemical analysis of KLK5 expression in control (*left panel*) OKF/6 cells or OKF/6 cells transfected with a KLK5 expression vector to generate OKF/6-KLK5+ cells (*right panel*). Cells were cultured on glass coverslips, fixed, and incubated with antibodies against KLK5 (1:50 dilution) followed by Alexa-Fluor-labeled secondary antibodies and counterstained with DAPI. Scale bar 100 μm. *B*, quantification of immunofluorescent staining with NIH ImageJ for average intensity. *C*, quantitative real time PCR analysis of KLK5 levels in control and KLK5+ OKF/6 cells. Relative quantification normalized against the housekeeping gene PGK-1 mRNA levels. Graph depicts KLK5 levels in OKF/6-KLK5+ cells normalized relative to OKF/6 parental cells (designated as 100). *D*, analysis of Dsg1 processing in OKF/6-KLK5+ cells. Lysates from parental OKF/6 cells (*lane 1*), vector-transfected OKF/6 cells (*lane 2*), and OKF/6-KLK5+ cells (*lane 3*) were electrophoresed on 9% SDS-polyacrylamide gels, transferred to PVDF membrane, and immunoblotted with anti-Dsg1 (1:1000; *upper panel*), anti-E-cadherin (1:1000; *middle panel*) or anti-GAPDH (1:4000; *lower panel*) followed by peroxidase-conjugated secondary antibody (1:4000) and peroxidase substrate. The *arrow* denotes migration position of full-length Dsg1 (165 kDa); *arrowhead* denotes migration position of cleavage product (~130 kDa). *E*, densitometric quantitation of band density of Dsg1 cleavage product denoted by *arrowhead* in *D*. *F*, densitometric quantitation of band density of corresponding blots shown in *D*.

tating single cell suspensions of SCC25 cells aggregated slowly (Fig. 6, *A* and *E*) and were present as small aggregates and single cells at 7 h of incubation (Fig. 6*F*). In contrast, KLK5 knockdown resulted in significant differences in aggregation kinetics detectable as early as 3 h (Fig. 6, *B* and *E* ($p < .05$), *G*), with highly significant differences observed at longer time points ($p < 0.001$). At 7 h, large multicellular aggregates were present with no visible single cells. Conversely, normal oral keratinocytes rapidly form robust aggregates (Fig. 6, *C*, *H*, *I*). However, introduction of KLK5 expression significantly delays aggregation kinetics as early as 3 h ($p < .05$), with highly significant differences observed at longer time points ($p < .001$). Similar to results observed in parental SCC25 cells, the majority of the OKF/6-KLK5+ population remains as single cells at 7 h (Fig. 6*J*).

To examine the relative resistance of epithelial cell sheets to dissociation into single cells, a dispase-based dissociation assay was used. Harvested cell monolayers were pulsed with dispase and subjected to controlled mechanical agitation followed by semi-quantitative analysis of sheet fragmentation

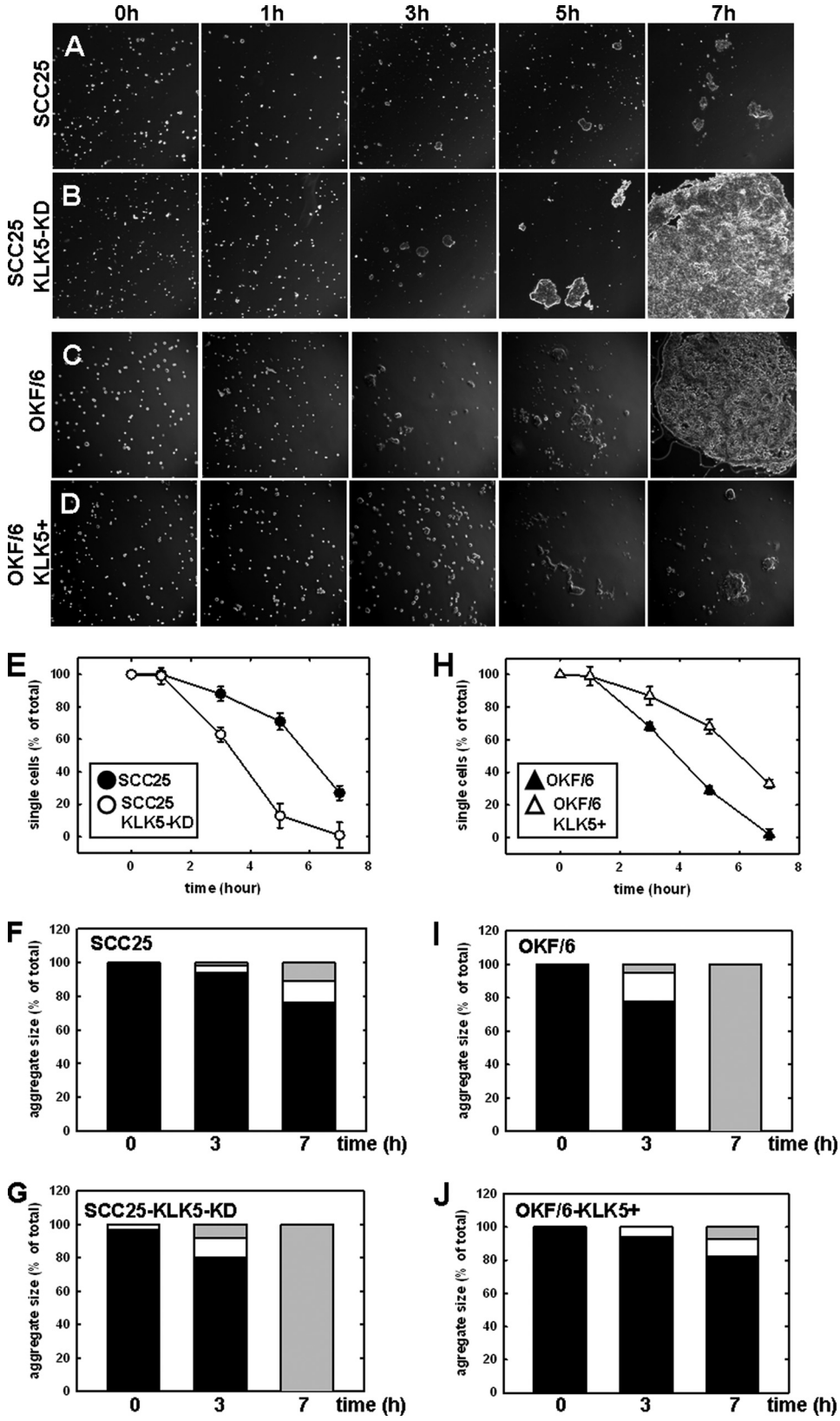

FIGURE 6. **Effect of KLK5 expression on cell-cell aggregation dynamics.** Single cell suspensions of (*A*) SCC25, (*B*) SCC25-KLK5-KD, (*C*) OKF/6, or (*D*) OKF/6-KLK5+ were incubated in culture medium containing 0.5% BSA and rotated for 7 h. At the indicated time points, aliquots were removed and photographed to visualize cell-cell aggregation. *E* and *H*, quantitation of aggregation kinetics. The number of single cells remaining in the suspension at each time point was enumerated and is shown relative to time 0 (100% single cells). (*Closed circle*) SCC25, (*open circle*) SCC25-KLK5-KD, (*closed triangle*) OKF/6, (*open triangle*) OKF/6-KLK5+. *F*, *G*, *I*, *J*, distribution of cellular aggregates. Within a high-powered field, the number of cellular clusters comprised of (*black bar*) <10 cells, (*white bar*) 10–50 cells, and (*gray bar*) >50 cells was enumerated at the designated time points. (*F*) SCC25, (*G*) SCC25-KLK5-KD, (*I*) OKF/6, (*J*) OKF/6-KLK5+.

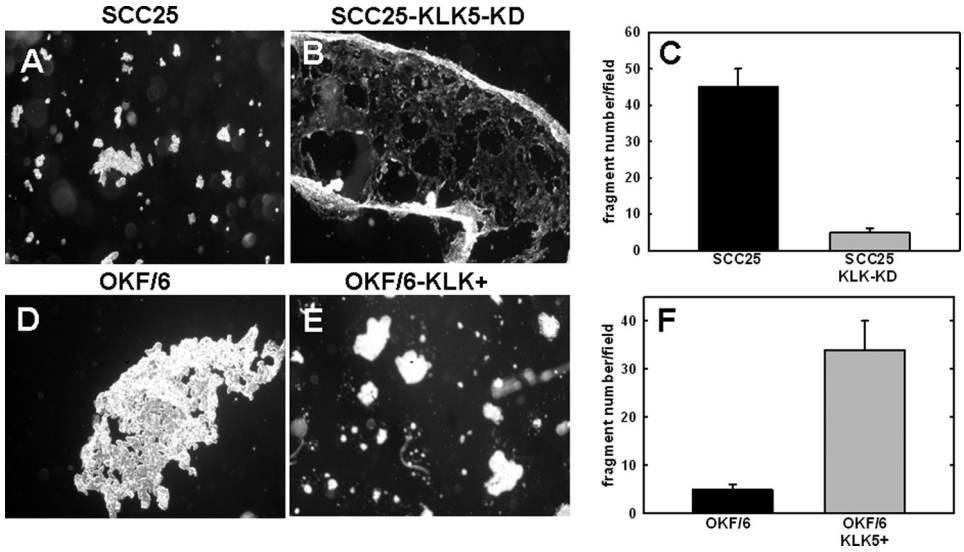

FIGURE 7. **Effect of KLK5 expression on monolayer cohesion.** Cell-cell adherent monolayers were separated from culture dishes by pulsing with dispase as described under "Experimental Procedures," transferred to conical tubes affixed to a rocking platform, and subjected to 50 inversion cycles**.** *A*, *B*, *D*, *E*, aliquots were photographed to visualize relative monolayer cohesion or dissociation. *C* and *F*, total number of fragments present following mechanical disruption was quantified.

(26, 39). SCC25 monolayers dissociated into numerous smaller fragments consistent with reduced epithelial cohesion (Fig. 7, *A* and *C*). In contrast, SCC25-KLK-KD cells retained better epithelial integrity, as evidenced by a 14-fold reduction in fragment number (Fig. 7, *B* and *C*). Conversely, OKF/6 cells remained largely clustered following dispase treatment (Fig. 7, *D* and *F*). However, introduction of KLK5 expression resulted in a relative 6-fold loss of cohesivity of OKF/6-KLK5+ aggregates (Fig. 7, *E* and *F*).

DISCUSSION

Human tissue KLKs are aberrantly expressed in multiple malignancies including those of the prostate, breast, and ovary (9–12). While accumulating data support the clinical utility of various KLKs as prognostic biomarkers in these cancers, KLK expression has not been extensively evaluated in OSCC. Using cDNA microarray screening of aggressive OSCC cells, combined with qPCR and immunohistochemical methods, we previously reported that KLK-5, -7, -8, and -10 are abundantly expressed in OSCC (8, 27). Further, a recent study correlates up-regulated KLK-4 and -7 expression with poor survival in OSCC patients (40). Although the potential functions of these KLKs are not fully elucidated, emerging data suggest that analysis of KLK expression may provide a useful clinical parameter for molecular classification of oral SCC lesions. Concurrent with up-regulation of KLKs in OSCC, aberrant staining of desmosomal components including desmogleins and desmocollins is also observed in human OSCC relative to normal oral mucosa (30, 31, 40). Data in the current study support these findings, showing both reduced staining intensity and loss of junctional localization for Dsg1 in a panel of human tongue tumors.

To test the hypothesis that KLK-5 may contribute to OSCC progression via modulation of cell-cell junctional integrity, in the current study the effect of KLK5 expression on Dsg1 processing was evaluated. Our results show that acquisition of KLK5 expression results in cleavage of Dsg-1, while processing of functionally related cell adhesion molecules including desmocollin-1, desmoglein-3 and E-cadherin was not observed. Dsg-1 proteolysis was associated with a corresponding loss of cell-cell adhesive function as assessed by transmission electron microscopy together with functional assays of cell-cell aggregation and dispersal. Indeed, down-regulation of KLK5 expression in malignant SCC25 cells significantly enforced cell-cell adhesion, as demonstrated by both cell-cell aggregation and dissociation assays. In contrast, overexpression of KLK5 in normal oral mucosal OKF/6 cells led to reduced cell-cell cohesion.

Cell-cell adhesion is an essential function that contributes to the maintenance of tissue integrity and barrier function (41, 42). Within the normal epidermis, desmosomes are present at extensive keratinocyte cell-cell contacts and provide strong intercellular adhesion. Desquamation, the process of shedding of superficial corneocytes, has been shown to involve KLK-mediated proteolytic processing of corneodesmosin, Dsg1, and desmocollin 1 (9, 14, 15). Direct cleavage of recombinant Dsg1 by KLK5 and identification of KLK5 cleavage sites in the Dsg1 extracellular domain have also been reported (32). KLK5-catalyzed Dsg1 cleavage occurs within the first three extracellular cadherin repeat domains (ECI-ECIII), which mediate heterophilic binding to desmocollins (32), suggesting that KLK5 action may destabilize Dsg1 structure and abolish adhesion to desmocollins on neighboring cells. Moreover, extracellular Dsg1 proteolytic fragments generated by KLK5 may further perturb intercellular adhesion by competing with intact Dsg1 and desmocollin 1 molecules for binding. Desquamation is further regulated by the protease inhibitor lympho-epithelial Kazal-type related inhibitor (LEKTI) encoded by SPINK5 (serine protease inhibitor Kazal-type 5) (43). Loss of LEKTI expression and/or function leads to dysregulated

proteolysis in the outer epidermal layers, loss of cell-cell cohesion, and defective barrier function (15). Interestingly, transcriptomic profiling has shown that expression of the SPINK5 gene is significantly down-regulated in human tongue tumors relative to normal tongue (44). Together with our report of up-regulated KLK5 expression in human tongue tumors (8) and the current results showing KLK5-mediated Dsg1 cleavage, these data suggest that KLK5 may potentiate metastatic dissemination of OSCC by contributing to dissolution of Dsg1-containing cell-cell contacts, thereby modifying epithelial cohesion.

Although our data implicate KLK5 activity in Dsg1 processing, the potential involvement of a downstream proteinase(s) that is activated by KLK5 cannot be ruled out using the current approach. Pro-KLK5 has been shown to undergo autoactivation and may process downstream zymogens including pro-KLK7 or other pro-KLKs (13, 45) that could functionally contribute to Dsg1 cleavage. Furthermore, it was recently demonstrated that the transmembrane serine proteinase matriptase, the zymogen of which undergoes highly efficient autolysis, functions to activate pro-KLKs *in vitro* and *in vivo* (46). As these data suggest the potential presence of a regulatory node further upstream in the zymogen activation cascade, future analysis of matriptase expression in OSCC is warranted.

REFERENCES

1. Jemal, A., Siegel, R., Zu, J., and Ward, E. (2010) *CA: Cancer J Clin.* **60,** 277–300
2. Sano, D., and Myers, J. N. (2007) *Can. Mets Rev.* **26,** 645–662
3. Rusthoven, K., Ballonoff, A., Raben, D., and Chen, C. (2008) *Cancer* **112,** 345–351
4. Horner, M. J., Ries, L. A., Krapcho, M., Neyman, N., Aminou, R., Howlader, N., Altekruse, S. F., Feuer, E. J., Huang, L., Mariotto, A., Miller, B. A., Lewis, D. R., Eisner, M. P., Stinchcomb, D. G., and Edwards, B. K. (2009) *SEER Cancer Statistics Review*, http://seen.cancer.gov/statistics
5. Shi, Z., and Stack, M. S. (2007) *Biochem. J.* **407,** 153–159
6. Shi, Z., and Stack, M. S. (2010) *Histol Histopathol* **25,** 917–932
7. Lundwall, A., Band, V., Blaber, M., Clements, J. A., Courty, Y., Diamandis, E. P., Fritz, H., Lilja, H., Malm, J., Maltais, L. J., Olsson, A. Y., Petraki, C., Scorilas, A., Sotiropoulou, G., Stenman, U. H., Stephan, C., Talieri, M., and Yousef, G. M. (2006) *Biol. Chem.* **387,** 637–641
8. Pettus, J. R., Johnson, J. J., Shi, Z., Davis, J. W., Koblinski, J., Ghosh, S., Liu, Y., Ravosa, M. J., Frazier, S., and Stack, M. S. (2009) *Histol. Histopathol.* **24,** 197–207
9. Borgoño, C. A., Michael, I. P., and Diamandis, E. P. (2004) *Mol Cancer Res.* **2,** 257–280
10. Lawrence, M. G., Lai, J., and Clements, J. A. (2010) *Endocr. Rev.* **31,** 407–446
11. Paliouras, M., Borgono, C., and Diamandis, E. P. (2007) *Cancer Letts.* **249,** 61–79
12. Pampalakis, G., and Sotiropoulou, G. (2007) *Biochim. Biophys. Acta* **1776,** 22–31
13. Michael, I. P., Pampalakis, G., Mikolajczyk, S. D., Malm, J., Sotiropoulou, G., and Diamandis, E. P. (2006) *J. Biol. Chem.* **281,** 12743–12750
14. Caubet, C., Jonca, N., Brattsand, M., Guerrin, M., Bernard, D., Schmidt, R., Egelrud, T., Simon, M., and Serre, G. (2004) *J. Invest. Dermatol.* **122,** 1235–1244
15. Descargues, P., Deraison, C., Prost, C., Fraitag, S., Mazereeuw-Hautier, J., D'Alessio, M., Ishida-Yamamoto, A., Bodemer, C., Zambruno, G., and Hovnanian, A., (2006) *J. Invest. Dermatol.* **126,** 1622–1632
16. Buxton, R. S., and Magee, A. I. (1992) *Sem. Cell Biol.* **3,** 157–167
17. Garrod, D. R. (1993) *Curr Opin Cell Biol.*, **5,** 30–40
18. Koch, P. J., and Franke, W. W. (1994) *Curr Opin Cell Biol.*, **6,** 682–687
19. Garrod, D., Chidgey, M., and North, A. (1996) *Curr Opin Cell Biol.* **8,** 670–678
20. Cheng, X., and Koch, P. J. (2004) *J. Dermatol.* **31,** 171–187
21. Rheinwald, J. G., and Beckett, M. A. (1981) *Cancer Res.* **41,** 1657–1663
22. Oda, D., Bigler, L., Lee, P., and Blanton, R. (1996) *Exp. Cell Res.* **226,** 164–169
23. Denning, M. F., Guy, S. G., Ellerbroek, S. M., Norvell, S. M., Kowalczyk, A. P., and Green, K. J. (1998) *Exp. Cell Res.* **239,** 50–59
24. Beynon, R., and Bond, J. S. (2001) *Proteolytic Enzymes*, pp. 320–323, Oxford University Press
25. Kowalczyk, A. P., Borgwardt, J. E., and Green, K. J. (1996) *J. Invest. Dermatol.* **107,** 293–300
26. Getsios, S., Amargo, E. V., Dusek, R. L., Ishii, K., Sheu, L., Godsel, L. M., and Green, K. J. (2004) *Int. Society Differ.* **72,** 419–433
27. Ghosh, S., Koblinski, J., Johnson, J., Liu, Y., Ericsson, A., Davis, J. W., Shi, Z., Ravosa, M. J., Crawford, S., Frazier, S., and Stack, M. S. (2010) *Mol. Can. Res.* **8,** 145–158
28. Arnemann, J., Sullivan, K. H., Magee, A. I., King, I. A., and Buxton, R. S., (1993) *J. Cell Sci.* **104,** 741–750
29. North, A. J., Bardsley, W. G., Hyam, J., Bornslaeger, E. A., Cordingley, H. C., Trinnaman, B., Hatzfeld, M., Green, K. J., Magee, A. I., and Garrod, D. R. (1999) *J. Cell Sci.* **112,** 4325–4336
30. Imai, K., Kumagai, S., Nakagawa, K., Yamamoto, E., Nakanishi, I., and Okada, Y. (1995) *Head Neck* **17,** 204–212
31. Harada, T., Shinohara, M., Nakamura, S., Shimada, M., and Oka, M. (1992) *Int. J. Oral Maxillofac. Surg.* **21,** 346–349
32. Borgoño, C. A., Michael, I. P., Komatsu, N., Jayakumar, A., Kapadia, R., Clayman, G. L., Sotiropoulou, G., and Diamandis, E. P. (2007) *J. Biol. Chem.* **282,** 3640–3652
33. Lundström, A., and Egelrud, T. (1988) *J. Invest. Dermatol.* **91,** 340–343
34. Lundström, A., and Egelrud, T. (1990) *J. Invest. Dermatol.* **94,** 216–220
35. Lundström, A., and Egelrud, T. (1990) *Arch Dermatol Res.* **282,** 234–237
36. Egelrud, T. (1993) *J. Invest. Dermatol.* **101,** 200–204
37. Ekholm, I. E., Brattsand, M., and Egelrud, T. (2000) *J. Invest. Dermatol.* **114,** 56–63
38. Egelrud, T., Brattsand, M., Kreutzmann, P., Walden, M., Vitzithum, K., Marx, U. C., Forssmann, W. G., and Mägert, H. J. (2005) *Br. J. Dermatol.* **153,** 1200–1203
39. Huen, A. C., Park, J. K., Godsel, L. M., and Green, K. J. (2002) *J. Cell Biol.* **159,** 1005–1017
40. Zhao, H., Dong, Y., Quan, J., Smith, R., Lam, A., Weinstein, S., Clements, J., Johnson, N. W., and Gao, J. (2010) *Head Neck*, in press
41. Green, K. J., and Gaudry, C. A. (2000) *Nat. Rev. Mol. Cell Biol.* **1,** 208–216
42. Candi, E., Schmidt, R., and Melino, G. (2005) *Nat. Rev. Mol. Cell Biol.* **6,** 328–340
43. Descargues, P., Deraison, C., Bonnart, C., Kreft, M., Kishibe, M., Ishida-Yamamoto, A., Elisa, P., Barrandon, Y., Zambruno, G., Sonnenberg, A., and Hovnanian, A. (2005) *Nat. Genet.* **37,** 56–65
44. Ye, H., Yu, T., Temam, S., Ziober, B. L., Wang, J., Schwartz, J. L., Mao, L., Wong, D. T., and Zhou, X. (2008) *BMC Genomics* **9,** 69–80
45. Brattsand, M., Stefansson, K., Lundh, C., Haasum, Y., and Egelrud, T. A. (2005) *J. Invest. Dermatol.* **124,** 198–203
46. Sales, K. U., Masedunskas, A., Bey, A. L., Rasmussen, A. L., Weigert, R., List, K., Szabo, R., Overbeek, P. A., and Bugge, T. H. (2010) *Nat. Genet.* **42,** 676–683